1-2014

Impacts of disturbance history on forest carbon stocks and fluxes: Merging satellite disturbance mapping with forest inventory data in a carbon cycle model framework

Christopher A. Williams
Clark University

G. James Collatz
NASA Goddard Space Flight Center

Jeffrey Masek
NASA Goddard Space Flight Center

Chengquan Huang
University of Maryland, College Park

Samuel N. Goward
University of Maryland, College Park

Remote Sensing of Environment 151 (2014) 57–71

Contents lists available at ScienceDirect

Remote Sensing of Environment

journal homepage: www.elsevier.com/locate/rse

Impacts of disturbance history on forest carbon stocks and fluxes: Merging satellite disturbance mapping with forest inventory data in a carbon cycle model framework

Christopher A. Williams [a,*], G. James Collatz [b], Jeffrey Masek [b], Chengquan Huang [c], Samuel N. Goward [c]

[a] Graduate School of Geography, Clark University, Worcester, MA, USA
[b] NASA Goddard Space Flight Center, Biospheric Sciences Laboratory, Greenbelt, MD, USA
[c] Department of Geography, University of Maryland, College Park, MD, USA

ARTICLE INFO

Article history:
Received 29 January 2013
Received in revised form 8 October 2013
Accepted 15 October 2013
Available online 2 December 2013

Keywords:
Net ecosystem productivity
Carbon sequestration
Landsat change detection
Forest inventory and analysis
Conterminous United States

ABSTRACT

Forest carbon stocks and fluxes are highly dynamic following stand-clearing disturbances from severe fire and harvest and this presents a significant challenge for continental carbon budget assessments. In this work we use forest inventory data to parameterize a carbon cycle model to represent post-disturbance carbon trajectories of carbon pools and fluxes for specific forest types growing in high and low site productivity class settings. We then apply these trajectories to landscapes and regions based on forest age distributions derived from either the FIA data or from Landsat time series stacks (1985–2006) for 54 representative scenes throughout most of the conterminous United States. We estimate the net carbon uptake in forests caused by post-disturbance growth and decomposition ("regrowth sink") for forested regions across the country. At the landscape scale, the prevailing condition of positive net ecosystem productivity (*NEP*) is in stark contrast to local patches with large sources, particularly in the west where fires and clear cuts create contiguous disturbed patches. At the continental scale, regional differences in disturbance rates reflect management patterns of high disturbance rates in the Southeastern and South Central states, and lower disturbance rates in the Northeast and Northern Lakes States. Despite low contemporary disturbance rates in the Northeast and Northern Lakes States (0.61 and 0.74% y^{-1}), the regrowth sink there remains of moderate to large strength (88 and 57 g C m^{-2} y^{-1}) owing to the continued legacy from historical clearing. Large regrowth sinks are also found in the Southeast, South Central, and Pacific Southwest regions (85, 86, and 95 g C m^{-2} y^{-1}) where disturbance rates also tend to be higher (1.59, 1.38, and 0.93% y^{-1}). Overall, the Landsat-derived disturbance rates are elevated relative to FIA-derived rates (1.19 versus 0.93% y^{-1}) particularly for western regions. The differences only modestly adjust regional- and continental-scale carbon budgets, reducing *NEP* from forest regrowth by about 8%.

1. Introduction

Forest disturbance is a widespread phenomenon across North America (Goetz et al., 2012) and can have profound impacts on a host of ecosystem services including carbon storage and uptake. Disturbances arise from a wide range of agents including harvests, insects, pathogens, fires, hurricanes and droughts. Many of these disturbance processes are episodic and highly variable in space and time, and there is growing indication of increased rates under the pressure of a changing climate (e.g. Allen et al., 2010). Thus, large-area monitoring is needed to identify which areas are being disturbed by what mechanisms, how rates of disturbance may be changing, and to assess impacts on a range of important services that forest ecosystems provide.

Satellite imagery is a powerful tool for monitoring disturbance area and post-disturbance recovery. Given its moderate resolution (~30 m) and long temporal coverage (since 1985, earlier for the MSS era), Landsat provides an unparalleled record of forest disturbance and regrowth dynamics (Cohen, Harmon, Wallin, & Fiorella, 1996; Cohen, Spies, & Fiorella, 1995; Cohen et al., 2002; Goward et al., 2008; Kennedy, Cohen, & Schroeder, 2007; Schroeder, Cohen, & Yang, 2007). This record is of great value for regional to continental assessments of forest change. For example, Landsat imagery has been used to construct maps of forest age for single scenes (approximately 180 × 180 km each) (Binford, Gholz, Starr, & Martin, 2006; Masek & Collatz, 2006) or even an entire region such as Oregon–California, (Law et al., 2004; Turner et al., 2007). This prior work identified challenges from low accuracy of mapped stand age and also offered too small a sample to quantify US or North American rates of change. The Landsat Ecosystem Disturbance Adaptive Processing System (LEDAPS) (Masek et al., 2008) offers a step in the right direction toward a wall-to-wall record of stand-clearing disturbances across North America though its most recent

* Corresponding author at: 950 Main Street, Worcester, MA 01610, USA. Tel.: +1 508 793 7323; fax: +1 508 793 8881.
E-mail address: cwilliams@clarku.edu (C.A. Williams).

0034-4257/$ – see front matter © 2013 Elsevier Inc. All rights reserved.
http://dx.doi.org/10.1016/j.rse.2013.10.034

generation offered a 5- to 10-year mapping interval which is too coarse to identify disturbances and track regrowth where the surface reflectance signal recovers quickly. The recent North American Forest Dynamics (NAFD) project (Goward et al., 2008) uses a sample of 50 Landsat scenes to quantify annual to biennial rates of forest disturbances across the conterminous US over the past two and a half decades (Fig. 1), with data available for five additional scenes used for algorithm development and testing. This paper combines the NAFD disturbance rates with other data to assess carbon impacts of recent disturbances across the conterminous US.

Forest inventory data can help to quantify the temporal dynamics of standing stock recovery following disturbance as they record biomass stocks with stand age. However, inventories have not typically monitored carbon belowground and correspondingly lack information on soil carbon and heterotrophic respiration, thus presenting an incomplete quantification of post-disturbance carbon dynamics. A more complete view can be obtained with ecosystem process models that simulate litter and soil carbon flows, especially when constrained to produce stock regrowth that is consistent with age–biomass relationships reported in forest inventories (Masek & Collatz, 2006; Song & Woodcock, 2003; Williams, Collatz, Masek, & Goward, 2012; Zaehle et al., 2006). Forest inventory data are also valuable for characterizing the area of forests in different age classes, particularly for large-scale, regional applications. However inventories sample only a small fraction of forested area and may have sizeable biases especially for local applications. This warrants the use of more complete, fine-resolution geospatial data, such as from the Landsat record, to expand beyond plots to regional and continental scales.

The analysis reported here combines strengths of the above approaches in a manner similar to the work of Cohen et al. (1996), Law et al. (2004), Masek and Collatz (2006), and Turner et al. (2007) to arrive at a more detailed and comprehensive assessment of the carbon consequences of past and present forest disturbance and regrowth across the conterminous United States. It offers one of the first demonstrations of merging national forest inventory data (and uncertainties) with a large-area satellite disturbance record and carbon cycle model to obtain regional and conterminous US estimates of carbon consequences. The basic method builds on our recent work (Williams et al., 2012) documenting post-disturbance carbon stock and flux trajectories for specific forest types and regions across the US as derived from an inventory-constrained carbon cycle model. This study adds another dimension by applying trajectories to landscapes with forest age maps obtained from a combination of forest inventory data and a Landsat disturbance detection product (Goward et al., 2008; Huang, Goward, Masek, et al., 2009; Huang, Goward, Schleeweis, et al., 2009; Huang et al., 2010a). Utilizing the disturbance maps of Goward et al. (2008) (Fig. 1), we apply this methodology to 54 Landsat scenes spread across the conterminous United States spanning its major forest type and climate settings. For comparison we apply the same approach using age distributions derived from the Forest Inventory and Analysis (FIA) database analysis of Williams et al. (2012) in place of the satellite-derived disturbances. We also apply results to all forestlands across the conterminous US to evaluate consistency of carbon balance estimates at the national level.

2. Methods

2.1. Overview

The core approach involved calculating regional and national disturbance rates, carbon fluxes, and carbon stocks based on the product of characteristic post-disturbance carbon flux and stock (Q_{afp}) specific to forest age, forest type, and site productivity class strata, with the area of land in each strata (A_{afp}), consistent with Williams et al. (2012). Region-total or national mass fluxes and stocks, as well as their uncertainties (δ, described further below), were calculated by summing over forest age, forest type, and productivity class strata, as

$$\begin{aligned} Q_{reg} &= \sum_a \sum_f \sum_p \left(Q_{afp} A_{afp} \right) \\ \delta Q_{reg} &= \sum_a \sum_f \sum_p \left(\delta Q_{afp} \delta A_{afp} \right) \end{aligned} \quad (1)$$

The area in each class was obtained in two ways and results are compared. The first relied solely on FIA data describing the area of forest land across strata. The second approach used a series of Landsat-based disturbance maps to estimate the area of land in younger age classes (<21 years) and then involved adjusting the FIA age histogram to characterize the age distribution of the remaining land classified as undisturbed in the Landsat record. Data sources for each step are described in the following Section 2.2.

In addition to regional and national assessments, we produced maps of carbon fluxes and stocks for each Landsat scene on a nominal 1 km × 1 km grid. Each grid cell (x,y) of area A_{cell} (~0.01 × 0.01°) was assigned a single forest type (e.g. Aspen–Birch) but with proportions

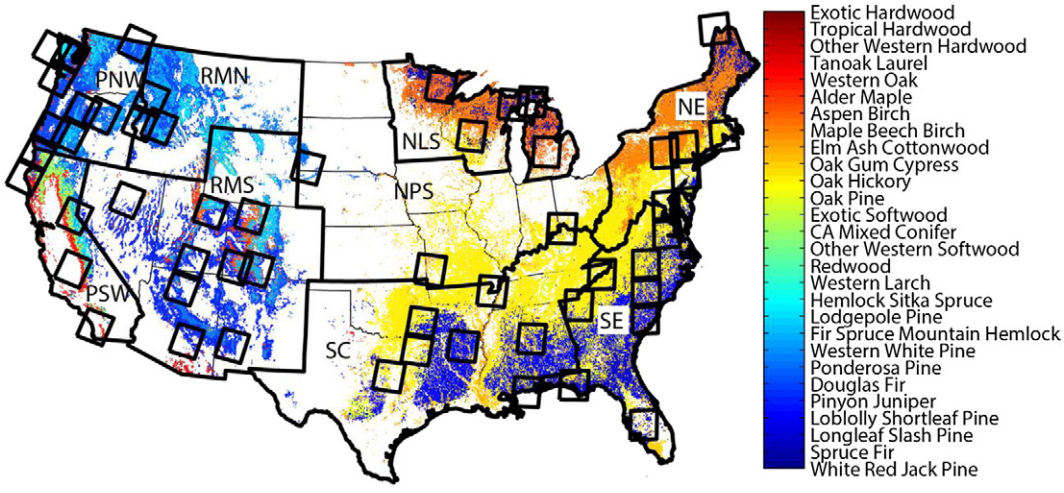

Fig. 1. Conterminous U.S. Forest Type Groups (Ruefenacht et al., 2008) shown with the distribution of Landsat scenes (squares) in NAFD sample. Thick state boundaries trace Forest Service regions. Colors loosely differentiate FIA forest type groups.

(F) within high or low productivity classes and of different stand ages, as

$$Q_{cell}(x,y) = \sum_{ap}\left(Q_{afp}F_{ap}(x,y)A_{cell}\right) \quad (2)$$

where subscripts are: a for stand age, f for forest type group, and p for productivity class. This approach allowed us to map carbon stocks (or biomass) as well as net ecosystem productivity (*NEP*), one of the key atmospheric flux components needed to understand carbon source/sink processes.

2.2. Data sources

Carbon flux and stock trajectories (see Fig. 2) were derived in our prior work (Williams et al., 2012) by fitting forest growth, decay, and allocation parameters within a modified version of the Carnegie–Ames–Stanford Approach (CASA) carbon-cycle process model (Potter et al., 1993; Randerson, Thompson, Malmstrom, Field, & Fung, 1996) to accumulate carbon in aboveground biomass consistent with forest inventory data. The model estimates net primary productivity (*NPP*), allocates *NPP* to live carbon pools including above and below ground biomass based on biome-specific rates, estimates mortality and shedding of live plant parts, simulates decomposition of dead carbon pools with individual turnover times and depending on litter quality assigned to each biome, and estimates associated heterotrophic respiration (*Rh*) based on the metabolic efficiency of the decomposer community. Seasonal phenology is imposed with a satellite-derived vegetation index (e.g. NDVI or fPAR). Productivity and decomposition rates are also influenced by temperature and moisture conditions. Net ecosystem productivity (*NEP*) is defined from the balance of net primary productivity (*NPP*) and heterotrophic respiration (*Rh*), where for the sake of simplicity the model neglects the generally smaller fluxes that contribute to the net carbon flux such as lateral fluxes of carbonate and organic matter in liquid form (see Chapin et al., 2006).

We modified CASA to capture disturbance impacts on the carbon cycle (Williams et al., 2012) such as: (1) post-disturbance decline and ensuing recovery of net primary production and fractional allocation to wood (τ) with an approach similar to that in past work (e.g. Amiro, Chen, & Liu, 2000; Hicke et al., 2003); and (2) disturbance-induced mortality of live wood, leaves, and roots. In this current modeling effort we assume that harvest clearings dominate the stand-replacing disturbance types and impose 85% to 95% mortality of live tree biomass akin to clearcut, seed tree, and high intensity shelterwood harvests that leave few residual trees. Similar to the approach in Turner, Koerper, Harmon, and Lee (1995), we remove 80% of disturbance-killed aboveground biomass with the remainder being treated as slash subject to decomposition as coarse woody debris left on site. This slash fraction is also consistent with Powell, Faulkner, Darr, Zhiliang, and MacCleery (1993) and Houghton and Hackler (2000). All leaves of disturbance killed trees are assumed to decompose on-site, modified from our prior work in which all leaves were removed. We introduced a new belowground coarse woody debris pool, and assume that all belowground wood that succumbs to mortality enters this pool before entering soil carbon pools (our prior work assumed that only 30% entered this CWD pool). Lastly, we slowed the rate of CWD turnover, which includes both fragmentation and decomposition processes, from an original effective rate of about 10% per year to a new rate of about 3% per year, depending on climate, to be more in line with rates reported for the region (Harmon et al., 1986; Laiho & Prescott, 2004). Modifications from our prior work (Williams et al., 2012) delay CWD release and correspondingly the time it takes for *NEP* to crossover from source to sink, but have a modest effect on continental and regional carbon budget estimates.

One of the most important alterations to the CASA model was joint adjustment to net primary productivity and mean residence time for live wood that allowed the best-match to the inventory data of aboveground stock recovery, as in Williams et al. (2012). Following determination of these parameters, characteristic carbon flux or stock trajectories (Q_{afp}) were developed from the following simulation sequence. We first simulated a 1000 year spin-up to steady-state carbon pools, and then imposed a stand clearing disturbance prior to the disturbance of interest, important in establishing the amount of live carbon subject to disturbance-induced disposition (taken off-site as removals or decomposing on-site). The stand age at harvest is set to be just older than the typical peak in age histograms reported by the FIA except where harvest rotations are known to be short such as in pine plantations of southern U.S. regions, or where harvest over previous decades tended to target old growth forests with high economic value (Cohen et al., 2002). This strategy yielded about 75 years of regrowth for all forest types except loblolly pine and longleaf/slash pine (30 years) and Douglas-fir (200 years). Last, we simulated the most recent disturbance after which we allow 200 years of regrowth to characterize carbon dynamics with stand development.

Inventory data were obtained from the FIA field plots (FIA Database Version 4), providing means and sampling errors for two attributes: 1) all live, oven-dry aboveground wood biomass, and 2) area of forest land. The quotient of these attributes provides biomass per unit area. Each attribute was sampled within strata of forest type group (28 classes), age (20 year age classes to 200+ years), and lumped into high and low productivity classes, defined from the rate of forest volume growth as 120 to >225 cubic feet acre^{-1} annum^{-1} and 20 to 119 cubic feet acre^{-1} annum^{-1} respectively. Inventory samples were drawn for nine regions defined by the Resource Planning Act (RPA) Assessment by the U.S.

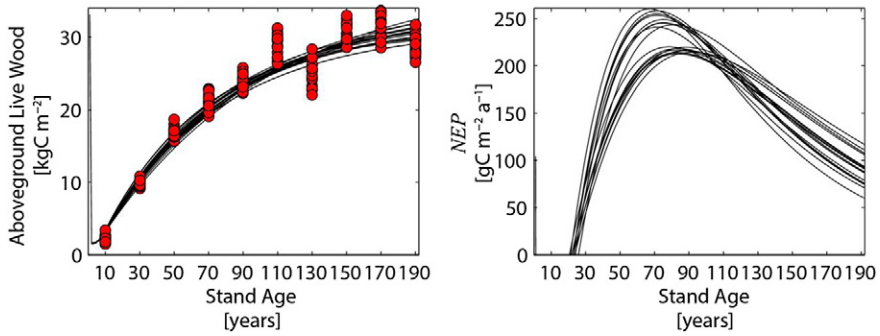

Fig. 2. Example characteristic trajectories of biomass regrowth and associated carbon sources/sinks (or net ecosystem productivity, *NEP*) following a stand-replacing disturbance in high productivity Douglas-fir stands of the Pacific Northwest. Results are from the CASA model fit to regrow stocks consistent with 25 independent samples from the forest inventory data (red circles). Net releases in the year following disturbance are as low as −1600 g C m^{-2} a^{-1} rising to above −500 g C m^{-2} a^{-1} in the second year of regrowth.

Forest Service that divides the conterminous US into the Northeast (NE), Southeast (SE), Northern Lakes States (NLS), South Central (SC), Northern Prairie States (NPS), Rocky Mountain North (RMN), Rocky Mountain South (RMS), Pacific Southwest (PSW), and Pacific Northwest (PNW) regions (Fig. 1). FIA data on forest carbon and area available via World Wide Web download include variances for each; however these uncertainties cannot formally be combined to estimate uncertainty in carbon stocks per unit area because of covariance between carbon stock and area (Bechtold & Patterson, 2005; Scott et al., 2005). To derive estimates (and variances) specifically for our regions of interest the USFS National Inventory and Monitoring Applications Center processed the national FIA plot data using the TabGen interface to provide our study with custom products that we employed in this analysis, namely the aboveground live wood biomass per unit area and its variance for each major forest type, stand age, and productivity class. Plot data were the target sample unit and statistics were calculated for those plots meeting the strata mentioned above. The database query involved both annual and periodic surveys and multiple survey years as reported in Appendix A. Data were filtered to include only single condition plots to avoid the possibility of partially disturbed segments of plots. The frequency of age-resetting disturbance was determined from the fraction of total forested area that is designated with a stand age of less than 20 years divided by 20 for forest types and productivity classes in each region.

The trajectories applied in this work are most representative of clearcut, seed tree, and high intensity shelterwood harvesting, all of which leave few, if any, residual live trees. Harvesting of this type is estimated to account for approximately 80% of stand-replacing disturbances across the conterminous US (Williams et al., 2012) based on comparison of two of the major stand-replacing disturbance agents active in western US forests. Of all burned area reported by the Monitoring Trends in Burn Severity database (Eidenshink et al., 2007) for the western US (2723 $km^2\ y^{-1}$ averaged 1984–2008), only about one quarter was of high severity (673 $km^2 y^{-1}$) and potentially stand replacing (Ghimire, Williams, Collatz, & Vanderhoof, 2012). Of all the timberland that experienced cutting from 2001 to 2005 in the western US (5712 $km^2\ y^{-1}$), about half was by clearcutting (2404 $km^2\ y^{-1}$) (Smith et al., 2009, Table 43). This indicates that of the major disturbance agents active in the western US, about 78% (= 2404/(2404 + 673)) of the stand-replacing events were from clearcutting while in the eastern US where high severity fires are less common, even more of the stand-replacing events were likely derived from forest clearing practices. This still leaves a potentially large role for partial or selective harvesting which is reported to comprise greater than 50% of all harvesting (Smith et al., 2009, Table 43) though the intensity of harvest for these partial treatments remains unclear and can include harvesting that leaves few residual trees. The present analysis focuses only on the stand-replacing disturbances, which is what is well represented by our age-accumulation approach and associated extension presented here using the Landsat disturbance mapping dataset. Detail on how carbon legacies vary with disturbance type has also not been incorporated in the present work but is the subject of our ongoing work and implications are discussed below.

Satellite-based estimates of the year of the most recent forest disturbance over large areas were obtained from the NAFD dataset (Goward et al., 2012). This dataset was produced from analysis of annual to biennial time-series of Landsat imagery for 54 forested scenes across the conterminous US (Table 1, Fig. 1). Landsat scenes were selected for inclusion with a probability-based sampling design with preferential inclusion of scenes having greater forested area and also to take advantage of Landsat stacks readily accessible to NAFD investigators based on prior work (Masek et al., 2013). The original NAFD sample of Landsat scenes was designed to represent mean disturbance rates in east and west strata of the conterminous US (Masek et al., 2013) but was further stratified in this study to address well-known regional variation in forest carbon stocks and fluxes in our analysis. With this use of the dataset at the regional level, sampling error cannot be quantified and we cannot diagnose associated bias in the regional samples. Nonetheless, the dataset offers an unprecedented view of recent rates of forest disturbance and associated carbon impacts at the regional scale.

Table 1
Landsat scenes included from phases I and II of the NAFD project, and associated annual forest disturbance rates derived from those data.

WRS-2 path/row	Assigned region	D rate [% y^{-1}]	WRS-2 path/row	Assigned region	D rate [% y^{-1}]
p12r27	NE	0.87	p27r38	SC	1.05
p12r31	NE	0.69	p33r30	RMS	1.72
p14r31	NE	0.48	p34r34	RMS	0.81
p14r32	NE	0.82	p34r37	RMS	0.39
p15r31	NE	0.47	p35r32	RMS	0.85
p15r33	NE	1.11	p35r34	RMS	0.80
p15r34	SE	1.64	p36r37	RMS	1.34
p16r35	SE	1.28	p37r32	RMS	0.67
p16r36	SE	1.98	p37r34	RMS	0.65
p16r37	SE	2.09	p37r35	RMS	0.55
p16r41	SE	2.33	p40r37	PSW	2.44
p18r35	SC	0.68	p41r29	RMN	0.82
p19r36	SE	1.17	p41r32	RMS	1.13
p19r39	SE	1.90	p42r28	RMN	1.03
p20r33	SC	0.78	p42r29	RMN	1.54
p21r30	NLS	0.83	p42r35	PSW	1.01
p21r37	SC	2.03	p43r33	PSW	0.35
p21r39	SC	1.86	p44r26	PNW	1.07
p22r28	NLS	0.57	p44r29	PNW	2.06
p23r28	NLS	0.61	p45r29	PNW	0.63
p23r35	SC	0.87	p45r30	PNW	0.80
p24r37	SC	1.75	p46r30	PNW	1.18
p25r29	NLS	1.04	p46r31	PSW	0.92
p26r34	SC	0.97	p46r32	PSW	0.87
p26r36	SC	2.02	p47r27	PNW	1.47
p26r37	SC	1.53	p47r28	PNW	1.72
p27r27	NLS	0.94	p48r27	PNW	1.01

For each Landsat scene, semi-annual forest disturbances were mapped using the Vegetation Change Tracker (VCT) algorithm (Goward et al., 2008; Huang, Goward, Masek, et al., 2009; Huang, Goward, Schleeweis, et al., 2009; Huang et al., 2010a). The algorithm is most sensitive to severe disturbances for which the majority of canopy cover is killed, and may miss partial harvest or relatively diffuse disturbances such as with early beetle outbreaks. It involves two primary steps. First, it performs single image masking and normalization to calculate an integrated forestness index based on each pixel's spectral departure from the multi-spectral signature of known forest in each pixel's neighborhood. It then analyzes each pixel's forest z-score across a time series of annual to biennial images, and identifies major disturbances when the z-score rises above a threshold value for at least two consecutive observation periods (at least 1 or 2 years). The dataset provides the year of disturbance at a nominal 30 m resolution for each Landsat scene (approximately 185 km × 185 km). The year of disturbance can be easily converted into stand age maps if we assume that forest regeneration begins immediately following disturbances. Though the stand age and time since disturbance are not equivalent (Bradford, Birdsey, Joyce, & Ryan, 2008), their general correspondence is unequivocal for severe, stand-replacing disturbances and was confirmed in the validation work of Thomas et al. (2011). As such, stand age is simply the difference between a year of interest and the year of the last disturbance, such as 2006 − 1985 = 21 year stand age in 2006.

A minimum mapping unit (MMU) of four contiguous disturbed pixels (0.32 ha) was applied to reduce false positive speckling that can be caused from residual image to image misregistration (Masek et al., 2013). Though this reduces errors of commission it does risk omissions of small area disturbances (one to three isolated pixels) and/or low severity disturbance events, and reduced the raw, 30 m mapping of disturbance events by an average of about 20% (range 10% to 50%). Details

on radiometric and geometric processing of the raw L1T (orthorectified at-sensor radiance) data files available from USGS EROS are presented by Huang, Goward, Masek, et al. (2009), including conversion to surface reflectance with the LEDAPS atmospheric correction package (Masek et al., 2006; Vermote, Tanre, Deuze, Herman, & Morcrette, 1997). For explanation of water, cloud, and cloud shadow identifications see Huang et al. (2010a, 2010b). Validation efforts for six scenes (Thomas et al., 2011) based on visual evaluation of Landsat TM imagery combined with high-resolution digital imagery yielded scene-level user's accuracies of ~65% to 90% for forest disturbance detection within 1 year of the reference. There were generally more errors of omission than commission (Thomas et al., 2011), again suggesting possible underestimation of actual disturbance rates.

Each of the 54 NAFD Landsat scenes was assigned to the RPA Forest Service region with which it overlaps the most (Fig. 1). Scenes were overlain by a map of forest type group specified at a 0.01° resolution based on the 2004 map generated by the USFS (Ruefenacht et al., 2008). Scenes were also overlain by maps of each cell's fractions of forest land in high and low productivity classes, specified based on a smoothed interpolation of county-level FIA data. The number of pixels in each forest type, productivity class, and age class (0 to 25 years in 1 year increments) was summed over scenes in the region and divided by the total number of pixels in each forest type and productivity class strata to provide a sample of the frequency of forested area in each age class. The remaining frequency (1 — total area disturbed in remote sensing product) was augmented by the FIA-derived age-histograms characteristic of each forest type (see Fig. 3 for example). The augmented frequency distribution was adjusted to sum to unity over age classes. These layers were used to produce scene-specific maps of fluxes and stocks circa 2006, produced at a ~1 km resolution (0.01° × 0.01°). Stand age was specified by aggregating the 30 m Landsat-based product to the cell (~1 km × 1 km) and then augmenting this with the FIA-derived age-histogram characteristic of the cell's particular forest type according to the regional samples described above.

2.3. Uncertainty analysis

As in Williams et al. (2012), formal propagation of uncertainty from sampling errors for forested area (±10 to 100%) and total aboveground live biomass (±10 to 100%), volume to carbon conversion (±7%), and inaccuracies in the disturbed area from Landsat (±10%) were all included. Flux and stock consequences of uncertainty in stock regrowth was propagated with a Monte Carlo procedure, analogous to Tier 2 uncertainty estimation in the IPCC Good Practice Guide (IPCC, 2000). The model was fit to 25 different biomass regrowth trajectories, where each trajectory was generated from random samples of the normally distributed aboveground biomass for each age class (25 draws of biomass per unit area from each of 10, 20-year age classes). An additional 7% uncertainty was used to account for tree volume to carbon conversion (Smith & Heath, 2001). Put together this method involved over 130,000 simulations of age-dependent dynamics of forest carbon fluxes and stocks. The uncertainty of forest area was derived from the FIA data plus an additional 10% associated with inaccuracies in the Landsat-derived ages as estimated based on the accuracy assessment by Thomas et al. (2011). Independent uncertainties in the product of flux or stock with area were combined as $\delta Q_{total} = \left(\frac{\delta Q_{afp}{}^2}{Q_{afp}{}^2} + \frac{\delta A_{afp}{}^2}{A_{afp}{}^2}\right)^{1/2}$ (Taylor, 1997). We assumed random error propagation such that uncertainty was added in quadrature over forest types, productivity classes, and ages, but simply added within regions or across the country. This uncertainty aggregation is analogous to a Tier 1 uncertainty described in the IPCC Good Practice Guide (IPCC, 2000).

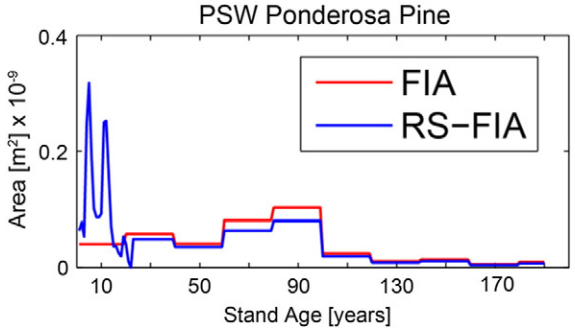

Fig. 3. Distribution of forest area by age for ponderosa pine of the PSW region comparing results from the FIA data alone or also including the remote sensing based (RS-FIA) estimates of recent age-resetting disturbances.

3. Results

3.1. Continental disturbance patterns

Forest disturbance rates vary greatly across scenes within regions (Table 1). As examples, rates in the Northeast range from 0.47 to 1.11% y^{-1}, in the Southeast they range from 1.28 to 2.33% y^{-1}, and in the Pacific Southwest they range from 0.35 to 2.44% y^{-1} (Table 1). This is consistent with expectation given the large variability of climate settings and associated forest types within regions, as well as sub-regional patterns in ownership (public or private lands), management, and vulnerability to as well as contingency upon the occurrence of natural disturbances. This is partly illustrated in Table 2, which reports disturbance rates for dominant forest types within each region. For example, in the Northeast region higher disturbance rates reported in softwood forests (pine, spruce, and fir forest types) is consistent with a larger fraction of total volume removed annually compared to that for hardwood forests (e.g. Oak and Hickory) (Smith et al., 2009). The same is true for the Southeast and South Central regions where disturbance rates are higher for softwoods than hardwoods, consistent with the much larger fraction of softwood volume (Longleaf and Slash Pine, Loblolly and Shortleaf Pine) that is harvested annually compared to hardwood volume (Oak Hickory and Oak Gum Cypress) (Smith et al., 2009). In the Northern Lakes States, where harvest removes a similar fraction of hardwood and softwood volumes (Smith et al., 2009), the remote sensing based analysis reports less variation in disturbance rates between forest types. One of the clear implications for regional and continental assessments of disturbance impacts is the need for large-area sampling to encompass these sources of variation.

The Landsat scenes selected for analysis by the NAFD project to date (in its first and second phases) effectively sample a broad range of the dominant forest types across each region (Table 3). This provides some justification for extrapolating the results from stacks within a region to the entire region and ultimately using the stacks to represent carbon dynamics for forests of the conterminous US. However, there are notable exceptions where samples are particularly limited, for example with White-Red-Jack Pine in the Northeast, Elm-Ash-Cottonwood in the Northern Lakes States, Aspen–Birch in the Pacific Southwest, and Pinyon–Juniper in the Rocky Mountain South (Table 3). Furthermore, the typical portion of total forest area sampled with the NAFD scenes is only about 10 to 30% of any given forest type within a region (Table 3). Any associated biases from under-represented forest types or from large-scale heterogeneity that could arise from a hurricane or unique state-level harvesting practices, for example, could yield a biased picture. Nonetheless, the NAFD sample combined with the FIA data offer the most extensive and detailed datasets available to assess disturbance rates and impacts.

Table 2
Area, disturbance rate, annual net ecosystem productivity, aboveground biomass (AGB), potential AGB at 200 years, and carbon storage potential in AGB for dominant forest types across regions of the conterminous US. Aboveground biomass is assumed to be 75% of the total live biomass for forests represented with the CASA model.

Region	Forest type	Area × 10^{-9}	Disturbance rate		Annual NEP		AGB		AGB at 200 years		C storage potential	
		[m^2]	[% y^{-1}]		[g C m^{-2}]		[kg C m^{-2}]		[kg C m^{-2}]		[Tg C]	
		–	FIA	RS	FIA	RS	FIA	RS	FIA	RS	FIA	RS
NE	WhiteRedJackP	20	0.66	0.11	93	92	8	8	11	11	50	50
NE	SprFir	28	0.75	0.96	51	36	5	5	10	10	141	143
NE	OakHic	93	0.23	0.54	126	115	9	8	16	16	660	697
NE	MapBeeBir	152	0.28	0.57	104	96	8	7	13	13	798	842
NLS	WhiteRedJackP	17	0.66	0.70	52	50	4	4	12	12	139	140
NLS	SprFir	31	0.28	0.61	34	30	3	3	4	4	39	43
NLS	OakHic	30	0.27	0.93	73	61	5	5	8	8	76	93
NLS	ElmAshCot	17	0.31	0.72	59	53	4	4	7	7	53	57
NLS	MapBeeBir	55	0.24	0.67	72	63	5	5	11	11	340	358
NLS	AspBir	51	1.21	0.61	44	53	3	4	7	7	196	177
SE	LongleafSlashP	40	2.30	1.83	28	44	4	4	8	8	174	162
SE	LobShort	91	2.34	1.80	106	124	5	5	12	12	653	607
SE	OakPine	40	1.61	1.54	58	59	5	5	13	13	332	329
SE	OakHic	123	1.08	1.36	74	65	6	6	11	11	577	614
SE	OakGumCyp	44	0.90	1.48	103	82	7	6	17	17	459	491
SC	LobShort	128	2.52	1.86	66	76	4	5	16	16	1517	1443
SC	OakPine	48	1.77	1.38	57	68	4	5	12	12	370	352
SC	OakHic	180	1.02	1.03	81	79	5	5	11	11	1000	1002
SC	OakGumCyp	46	0.70	1.37	111	81	7	6	13	13	274	309
SC	ElmAshCot	25	1.14	0.82	77	89	5	5	14	14	225	216
RMN	DougFir	60	0.58	1.37	32	17	5	4	15	15	591	635
RMN	PonderosaP	20	0.62	1.70	34	21	4	3	12	12	162	179
RMN	FirSprMtnHem	48	0.77	1.23	41	34	5	5	13	13	371	392
RMN	LodgepoleP	29	0.90	1.29	42	28	5	4	10	10	147	157
RMS	PinJun	220	0.14	1.31	10	7	1	1	2	2	165	222
RMS	DougFir	27	0.15	0.73	37	28	5	4	7	7	57	70
RMS	PonderosaP	53	0.14	1.37	36	19	4	3	5	5	67	111
RMS	FirSprMtnHem	62	0.26	0.50	48	45	6	6	9	9	196	211
RMS	LodgepoleP	29	0.73	0.55	42	43	5	5	8	8	91	86
RMS	AspBir	34	0.59	0.75	43	41	4	4	10	10	191	196
RMS	WestOak	37	3.38	1.42	−4	14	1	2	6	6	182	153
PSW	PonderosaP	12	0.51	1.45	53	40	5	4	15	15	123	134
PSW	FirSprMtnHem	11	0.11	0.42	128	113	13	12	23	23	111	121
PSW	CaMixCon	33	0.07	0.68	95	72	9	8	14	14	149	188
PSW	AspBir	12	0.31	0.09	137	142	14	14	14	14	0	0
PSW	WestOak	19	0.20	1.11	71	56	6	5	12	12	106	125
PSW	TanoakLaurel	7	0.36	0.83	151	132	12	11	15	15	24	30
PSW	OthWestHdwd	7	0.28	0.98	71	62	6	5	8	8	14	18
PNW	DougFir	81	0.80	1.30	50	41	11	11	25	25	1130	1173
PNW	PonderosaP	31	0.50	1.88	46	30	4	3	11	11	214	248
PNW	FirSprMtnHem	30	0.36	0.87	88	77	9	8	19	19	304	330
PNW	ElmAshCot	11	1.29	1.85	52	48	7	6	17	17	105	119
PNW	HemSitkaSpr	1	0.48	1.35	84	62	13	11	25	25	13	15
PNW	AlderMaple	13	1.21	1.94	91	87	8	7	16	16	110	119

Continental-scale patterns in the rate of forest disturbance across regions show some broad similarities between the NAFD-based and FIA-based estimates (Table 4). Disturbance rates tend to be lower in the Northeast and Northern Lakes States regions, and higher in the Southeast and South Central regions. However, in the Northeast region the remotely-sensed approach estimates nearly twice the rate of disturbance estimated from the FIA-based approach (0.61 versus 0.36% y^{-1}). Furthermore, approaches strongly disagree in western regions, with much higher rates recorded with the NAFD-based approach, for all of the PNW, PSW, RMN, and RMS regions (Table 4). The remote sensing analysis suggests rates that are 1.5 to 3 times greater than estimated from the FIA stand age data. In general, the remotely sensed based analysis suggests elevated rates of disturbance than we infer from the stand age attribute reported in the FIA database. We note that regional disturbance rates reported in Table 4 are not simply the average of scene-specific results for each region as presented in Table 3 because scene-level results are aggregated to the region with weighting by the fractional area of each forest type by productivity class stratum.

3.2. Continental patterns in forest carbon stocks and fluxes

The typical pattern of *NEP* following a stand clearing disturbance involves a large negative value immediately after disturbance when *NPP* is much reduced and *Rh* is elevated from fresh inputs of litter and woody debris (including roots of killed trees). This is followed by a 10 to 40 year rise in *NEP* to a maximum rate of carbon uptake and then a gradual decline as carbon inputs from productivity are balanced by carbon releases from respiration (Fig. 2). The magnitudes of net release and uptake and the timing of crossover from source to sink depends on the type of disturbance. As explained above, our method primarily represents the carbon dynamics post-harvest, which dominates the stand-replacing disturbances that take place across the US. In the discussion section we discuss how other disturbance types impact carbon transfers and the likely effects on both local and national *NEP* and Net Biome Productivity (*NBP*).

When the local carbon stock and flux dynamic is applied to landscapes, what becomes especially important is how much forestland is occupied by very young forests just recovering from a recent disturbance

Table 3
Fraction of region-wide forest area sampled in the NAFD 54-scene sample for dominant forest types. Area is reported in 10^9 m^2.

Region	Forest type group	Area in region	Area in NAFD sample	Fraction of area sampled
NE	WhiteRedJackP	20	0.6	0.03
NE	SprFir	28	3.5	0.12
NE	OakHic	93	35.2	0.38
NE	MapBeeBir	152	36.4	0.24
NLS	WhiteRedJackP	17	5.3	0.31
NLS	SprFir	31	10.3	0.34
NLS	OakHic	30	5.7	0.19
NLS	ElmAshCot	17	0.5	0.03
NLS	MapBeeBir	55	10.5	0.19
NLS	AspBir	51	16.4	0.32
SE	LongleafSlashP	40	9.8	0.24
SE	LobShort	91	34.4	0.38
SE	OakPine	40	4.2	0.10
SE	OakHic	123	44.4	0.36
SE	OakGumCyp	44	11.9	0.27
SC	LobShort	128	37.7	0.29
SC	OakPine	48	6.1	0.13
SC	OakHic	180	47.9	0.27
SC	OakGumCyp	46	9.5	0.21
SC	ElmAshCot	25	2.4	0.10
RMN	DougFir	60	15.9	0.27
RMN	PonderosaP	20	3.3	0.16
RMN	FirSprMtnHem	48	14.1	0.29
RMN	LodgepoleP	29	3.2	0.11
RMS	PinJun	220	4.2	0.02
RMS	DougFir	27	1.0	0.04
RMS	PonderosaP	53	7.3	0.14
RMS	FirSprMtnHem	62	10.6	0.17
RMS	LodgepoleP	29	3.0	0.10
RMS	AspBir	34	8.3	0.24
RMS	WestOak	37	2.6	0.07
PSW	PonderosaP	12	0.9	0.08
PSW	FirSprMtnHem	11	1.8	0.16
PSW	CaMixCon	33	12.3	0.38
PSW	AspBir	12	0.0	0.00
PSW	WestOak	19	4.3	0.22
PSW	TanoakLaurel	7	4.6	0.65
PSW	OthWestHdwd	7	0.2	0.03
PNW	DougFir	81	60.9	0.75
PNW	PonderosaP	31	10.9	0.35
PNW	FirSprMtnHem	30	8.2	0.27
PNW	ElmAshCot	11	2.1	0.19
PNW	HemSitkaSpr	1	0.0	0.03
PNW	AlderMaple	13	3.7	0.29

and for which *NEP* is still a large negative value or near neutral. A higher disturbance rate inevitably places more forestland in the youngest age classes with a typical net release of carbon, but if that rate of disturbance has been steady for the past few decades, a higher rate may also stimulate a larger area undergoing vigorous regrowth with the largest rates of *NEP*, potentially offsetting or even overwhelming releases from forestlands most recently disturbed.

Elevated rates of disturbance estimated with the remote sensing product compared to the FIA data translates to modestly reduced sink strengths for each region (*NEP*, Table 4). In the western regions in particular we find that the FIA-inferred disturbance rate tends to be lower than that derived from remote sensing. It is possible that country-wide variation in inventory practices contribute to this result. For example, the western states of CA, OR, and WA historically used a periodic inventory design with a variable-radius plot with five subplots in contrast to the annual inventory approach of a fixed plot size and four subplots used in more eastern states. In the periodic design, subplots are more spread out and sample a larger amount of land which could decrease the likelihood of recording a young stand age given that disturbances tend to be spatially localized. This would tend to decrease the rate of disturbance inferred for western states that continued to employ the periodic inventory approach until the more recent shift toward the fixed plot, annual inventory design.

At a regional-scale we find net carbon uptake in forests (*NEP*, Table 4) caused by post-disturbance growth that outweighs release from decomposition, thus defined as a "regrowth sink". It is important to note that this refers specifically to the carbon balance within forested lands, not the full forest sector which also includes the fate of wood products (we include additional terms elsewhere). This term results from the balance of *NPP* and *Rh* as they change over time following a clearcut disturbance, including growth of all vegetation from surviving trees (if any) and regeneration from resprouts, saplings, or seedlings, as well as heterotrophic respiration from detritus present before disturbance, disturbance-killed detritus, and detritus formed newly from mortality of regeneration in the post-disturbance period. In this work we have not sought to disaggregate these *Rh* components within our modeling framework. While the sign of corresponding *NEP* is not always >0 as the term "sink" implies, the aggregate regional to continental scale *NEP* is positive as growth (or regrowth following disturbance) exceeds release through decomposition.

As we reported in our prior work, regrowth sinks in the Northeast and Northern Lakes States remain of moderate to large strength (94 and 52 g C m^{-2} y^{-1}, respectively for RS-based results in Table 4) despite lower contemporary rates of disturbance. This is owing to the continued regrowth legacy from historical clearing across these northern regions. Regrowth sinks are also large in the Southeast, South Central, Pacific Northwest and Pacific Southwest regions (55 to 87 g C m^{-2} y^{-1} for RS-based results). Sinks are much smaller in the Rocky Mountain regions at only about 20 g C m^{-2} y^{-1}, despite some of the country's highest disturbance rates, particularly in the Rocky Mountain North (1.52% y^{-1}, Table 4). Forest recovery tends to be relatively slow in the southern dry and northern cold Rocky Mountains.

Table 4
Regional results for forested area, net ecosystem productivity (*NEP*), above- plus below-ground live biomass (Live *B*), rate of forest disturbance per year for the period 1986 to 2005 (D rate), annual harvest removals, and net biome productivity (*NBP* = *NEP* – Harvest). Subheadings RS and FIA refer to results when age distributions are estimated either with or without the NAFD 54-scene Landsat product.

Region	Area	*NEP* [TgC y^{-1}]		Live *B* [PgC]		D rate [% y^{-1}]		Harvest [TgC y^{-1}]		*NBP* [TgC y^{-1}]	
	[10^9 m^2]	RS	FIA	RS	FIA	RS	FIA	RS	FIA	RS	FIA
NE	339	32 ± 4.6	35 ± 4.7	3.3	3.4	0.61	0.36	20	8	12	27
NLS	211	11 ± 1.1	12 ± 1.2	1.1	1.1	0.74	0.59	8	5	3	7
SE	354	28 ± 3.4	28 ± 2.8	2.5	2.6	1.59	1.60	28	31	0	−3
SC	456	35 ± 4.4	34 ± 3.3	3.1	3.0	1.38	1.55	38	38	−3	−4
RMN	192	4 ± 1.1	6 ± 1.3	1.1	1.2	1.52	1.04	17	10	−13	−4
RMS	493	9 ± 5.3	11 ± 5.2	1.7	1.8	1.15	0.58	10	9	−1	2
PSW	127	11 ± 2.5	13 ± 2.7	1.5	1.6	0.93	0.38	9	3	2	10
PNW	202	11 ± 2.7	14 ± 2.7	2.2	2.4	1.43	0.73	23	22	−12	−8
Total/mean*	2374	141 ± 25	152 ± 24	16.6	17.2	1.19	0.93	153	126	−12	26

* Forest-area weighted mean of regional disturbance rates.

The annual removal of biomass carbon through harvesting is as large as or larger than *NEP* (Table 4). Harvested biomass is delivered to wood products (paper, pulpwood, saw logs, veneer logs, composites, fuel wood, etc.) and each product has its own disposition, rate of turnover, and emission but much of it is ultimately released back to the atmosphere as CO_2 or CH_4 over the ensuing decades (Skog & Nicholson, 1998). Half-lifes range from a century for single-family homes to only a year for paper. Though it is beyond the scope of the current work to calculate the carbon emissions and storage in wood products, we can approximate the full forest sector carbon balance by quantifying *NBP* from the difference of *NEP* within forests and annual removals by harvest (Table 4). Subtracting the rate of removals we find that harvesting of conterminous US forests yields a near zero carbon balance ranging from a small net carbon source to a small sink of about −12 to 26 TgC y^{-1} for RS- and FIA-based estimates.

Live biomass stocks can be a better indicator of how local and regional carbon balances respond to disturbances because they record the transfers from live to dead pools and/or removals through combustion or harvest. Forest carbon stocks are relatively high in the Northeast, Pacific Southwest, and Pacific Northwest regions, averaging about 11 to 12 kg C m^{-2} or more (Table 4, Live *B* divided by forest area). Live biomass stocks are low on average across the Rocky Mountain regions (3 to 6 kg C m^{-2}), and also across the Southeast and South Central regions (7 kg C m^{-2}) because of vigorous harvesting.

What may best reveal the carbon impacts of disturbances is the difference between actual and potential live biomass stocks. For example, though the current stocks in Pacific regions are relatively high compared to much of the country, the potential carbon stocks can be far higher, particularly where aboveground biomass alone can reach 20 to 25 kg C m^{-2} (Table 2). Thus it is most instructive to study the current stock relative to the potential stock at some fairly mature stage such as at 200 years since the last disturbance. This is reported in Table 2 as the carbon stock potential for dominant forest types of each region, and also summarized by region and across the country in Table 5. Carbon storage potential from (re)growth is large in the areas where harvesting is most active, including the Southeast, South Central, Pacific Northwest and Pacific Southwest regions, partly reflecting how much biomass removal has taken place in the recent years/decades. Adjusting for the area of each region, we find that the Rocky Mountain North has relatively high carbon storage potential (11 kg C m^{-2}) not because of a high potential forest biomass stock (17 kg C m^{-2}) but because its current biomass stocks are so low (6 kg Cm^{-2}) given the region's high rates of disturbance. The South Central region has similar results on a per area basis. Though current biomass stocks are relatively high in the Pacific Northwest on average (11 to 12 kg C m^{-2}), the region's potential biomass stock is much greater at about 25 kg C m^{-2} and thus it has the greatest capacity for carbon storage on a per unit area basis (14 kg C m^{-2}). On average, regions hold about 47% of their potential forest carbon stocks, with a low of 34% in the Rocky Mountain North and high of about 58% in Northeast and Pacific Southwest regions. Considering the country scale, if all of the conterminous US forestland was capable of holding its 200-year potential live biomass stock at the same moment in time we estimate there would be at least an additional 19 Pg C stored in forests of the conterminous US (Table 5).

Lastly, we examine how *NEP* today (circa 2006) is responding to just the most recent disturbances over the prior two decades (Table 6). Region-integrated *NEP* responses to the past two decades of disturbances are close to 0 Tg C y^{-1} but negative and add up to a modest source for the conterminous US (−16 to −8 Tg C y^{-1}). The large carbon releases immediately after disturbances are weakly opposed by modest net carbon uptake from forest regrowth, with a crossover from source to sink typically occurring within 10 to 15 years post-disturbance though it can be as long as 30 years for forests with a large amount of coarse woody debris and relatively slow regrowth (e.g. harvest of old-growth Douglas-fir in the Pacific Northwest). It is important to note that this does not consider the release of carbon assumed to have been removed from disturbed patches (akin to harvest or severe fire), as *NEP* only includes the biologic balance of uptake from productivity and release from respiration and does not include emissions from fires or decomposition of harvested wood products. For this youngest fraction of forestlands (<25 years old), elevated disturbance rates obtained from the NAFD product compared to that inferred from FIA data yields a country-wide net carbon release of about 8 Tg C y^{-1} because a larger fraction of forest is assigned to the youngest ages where *NEP* is negative to neutral. Considering forestlands of all ages, the elevated RS-based disturbance rates reduce the country's forest regrowth sink by about 7% (152 reduced to 141 Tg C y^{-1}, Table 4).

Table 6
Net ecosystem productivity (*NEP* Young Stands [Tg C y^{-1}]) for all stands in the 0 to 24 year age class by region.

Region	*NEP* young stands	
	RS	FIA
NE	−1	0
NLS	−1	0
SE	−1	0
SC	−5	−2
RMN	−2	−1
RMS	−2	−1
PSW	−1	0
PNW	−4	−4
Total	−16	−8

Table 5
Regional live biomass (Live *B*), live biomass if all forests were at least 200 years old (Live *B* 200 years), and carbon storage potential in live biomass (C storage potential) all in units of [Pg C]. Subheadings RS and FIA refer to results when age distributions are estimated either with or without the NAFD 54-scene Landsat product.

Region	Live *B* 200 years	Live *B*		C storage potential	
	–	RS	FIA	RS	FIA
NE	6.0	3.3	3.4	2.7	2.6
NLS	2.3	1.1	1.1	1.2	1.2
SE	5.6	2.5	2.6	3.1	3.1
SC	7.8	3.1	3.0	4.7	4.8
RMN	3.2	1.1	1.2	2.1	2.0
RMS	3.2	1.7	1.8	1.5	1.4
PSW	2.6	1.5	1.6	1.1	1.0
PNW	5.2	2.2	2.4	3.0	2.8
Total	35.9	16.5	17.2	19.4	18.7

3.3. Scene-specific maps

Mapping disturbance year and associated carbon impacts reveal valuable insights into the underlying processes and the nature of how it is imposed upon other sources of spatial variation such as forest type and climate. Figs. 4, 5, and 6 provide example scenes showing the year of most recent disturbance at 30 m resolutions. Many of the disturbances are patch-scale and correspondingly diffuse and dispersed across the landscape often with regular shaped perimeters indicating ownership or management boundaries. These typically correspond to harvest events. However, for the scene in the Sierra Mountains of California (Fig. 6), immediately evident are the imprints of large-scale disturbance events that create contiguous patches with irregular perimeters. Such patches are typically the signature of major fires, as has been verified by an overlay of the USGS Monitoring Trends in Burn Severity (MTBS) dataset (Eidenshink et al., 2007).

Combining stand age maps with those for forest type group, productivity class, as well as flux/stock trajectories we obtain geospatial carbon

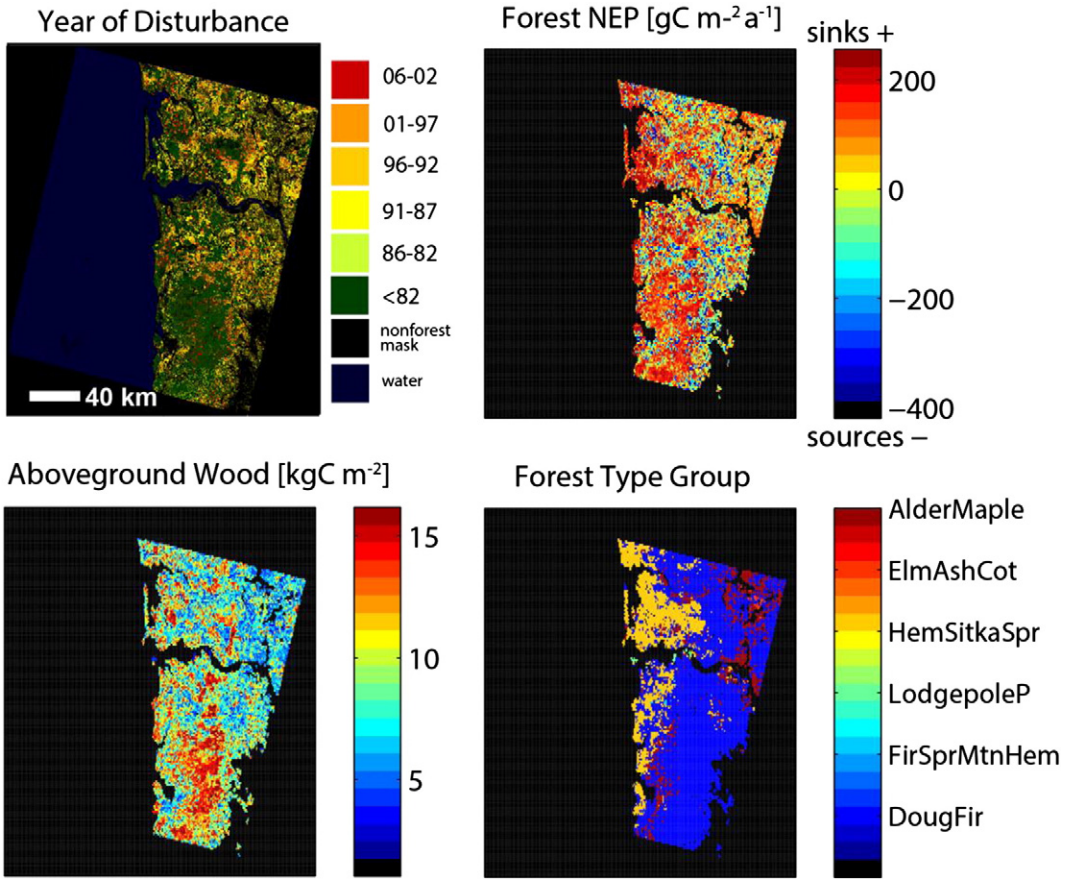

Fig. 4. Maps of year of disturbance (Goward et al., 2008), net ecosystem productivity (*NEP*), aboveground wood, and forest type group for Landsat scene p47r28 located on the Pacific Northwest coast. Stocks and fluxes are for the year 2006. Disturbance year imposes a clear imprint on forest NEP and aboveground woody biomass, with residual association to forest type group.

flux and stock maps. Figs. 4–6 offer examples for which the data density was coarsened to a 1 km × 1 km scale, indicating the average or sum of contributions at the 30 m × 30 m scale. These carbon flux and stock estimates are spatially explicit only for those pixels or portions of pixels that experienced stand-replacing disturbance within the Landsat record studied here (1985–2005). Estimates elsewhere are assigned the average flux or stock of more mature forests. Spatial variations in aboveground biomass and net primary productivity are clearly influenced by the distribution of forest types. In contrast net ecosystem productivity is more strongly linked to stand age, with large sources in recently disturbed tracts and sizeable sinks in young (e.g. 30 year), vigorously regenerating forests. Such detailed mapping of carbon flux patterns has great potential to contribute to regional and continental scale carbon budgets, offering unique consideration of stand age, forest type, and productivity class based on a novel merger of a carbon balance model, remotely sensed disturbances and forest inventory data.

4. Discussion

It remains unclear why the area of forest within FIA stand age classes generally yields lower disturbance rates than those of the Landsat analysis. One possibility is that national scale use of the FIA data includes historic heterogeneity in sampling procedures that may introduce regional variation in sampling extent potentially introducing errors or bias in the representation of the frequency distribution of stands of different ages. In regions that have a lower density of plot samples, such as was common for implementation in some western states, punctuated, rare disturbance events will be less well represented. Furthermore, the fixed, periodic plot design used historically in western states, which involved data collection in large, contiguous blocks, may have provided a less representative sample of the full landscape and this might explain the generally poorer agreement between FIA and RS derived disturbance rates for western compared to eastern regions. This underscores the value of and need for continental-scale, continuous maps of disturbances derived from remote sensing, such as being developed with the continuing NAFD effort. Another possibility is an issue of scale associated with the size of individual plots sampled in the FIA approach or the method of determining and assigning stand age to plots. In the FIA database stand age is often determined from tree-ring dating of live trees cored with an increment borer in the field and the sampled trees are appropriately selected to be representative of older individuals on the plot, however it is sometimes computed based simply on the number of years since the last survey if the stand has not been seriously disturbed since then. In addition, the plot data used in this analysis were intentionally filtered to include only single condition plots to avoid the possibility of partially disturbed segments of plots. However, it is possible that this imposes a spatial filter on the scale of stand clearings that could be sampled, with a low probability of an entire plot being cleared by a single disturbance. On the other hand, some of the Landsat-detected disturbances are representative of partial clearings that do not reset stand age such that the use of the data product in this study may overestimate the rate of stand-clearing disturbances. Validation efforts have indicated that the Vegetation Change Tracker algorithm includes some partial disturbances that do not kill the majority of trees within a pixel (Huang, Goward, Schleeweis, et al., 2009; Thomas et al.,

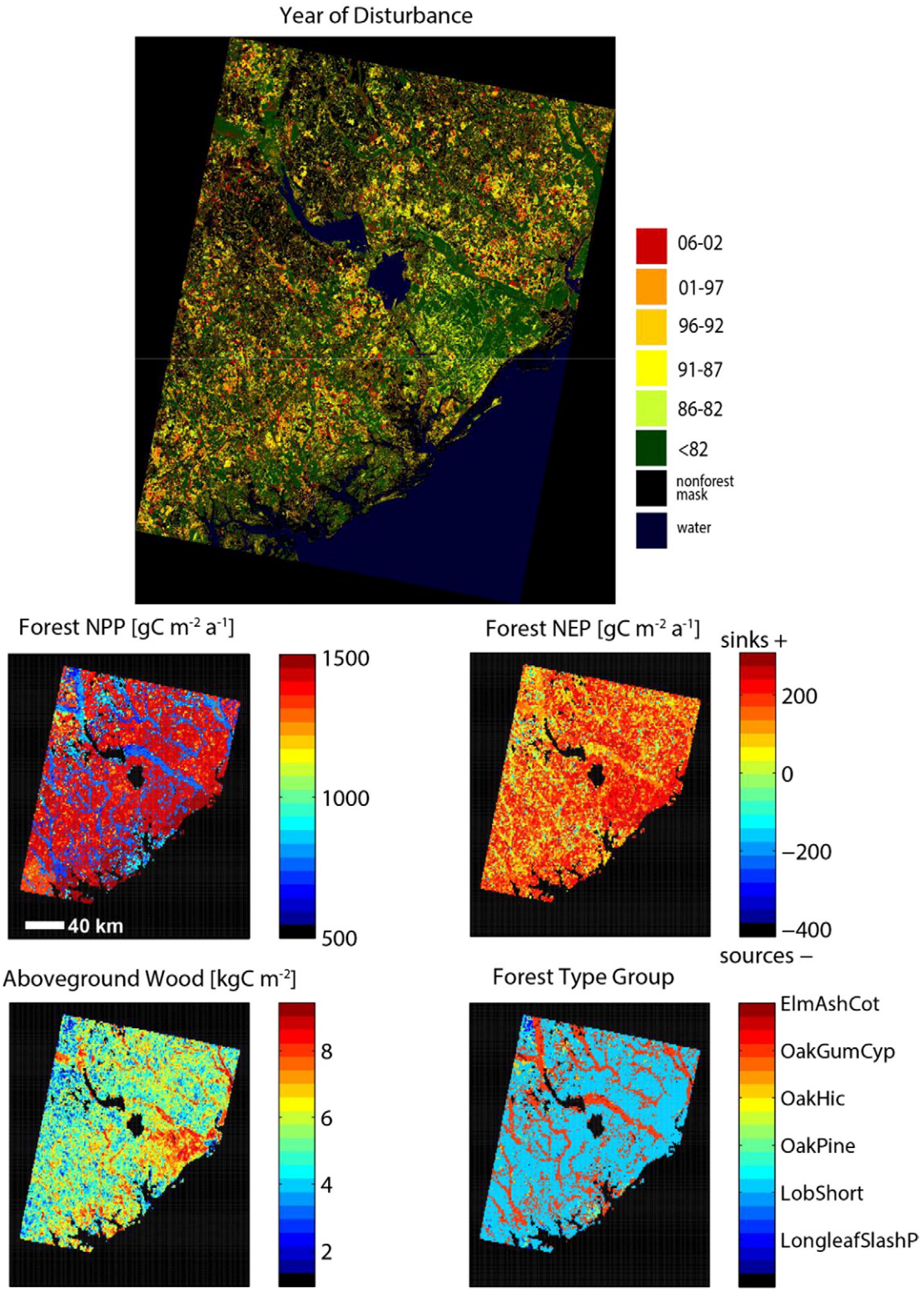

Fig. 5. Maps of year of disturbance, net primary productivity (*NPP*), net ecosystem productivity (*NEP*), aboveground wood, and forest type group for Landsat scene p16r37 located on the Southeastern coast of the Carolinas.

2011). The current generation of NAFD products does not clarify which disturbed pixels experienced low to moderate severity disturbance or partial clearing and which experienced severe or stand-clearing disturbance and if feasible this would be a helpful addition. With large areas of forest affected by selective harvesting or partial mortality events from beetles and low to moderate severity fires (Smith et al., 2009), future work should develop methods that more fully account for associated impacts.

In this work we represented the carbon impacts of disturbances in terms of both *NEP* and carbon stocks. Both are important but potentially

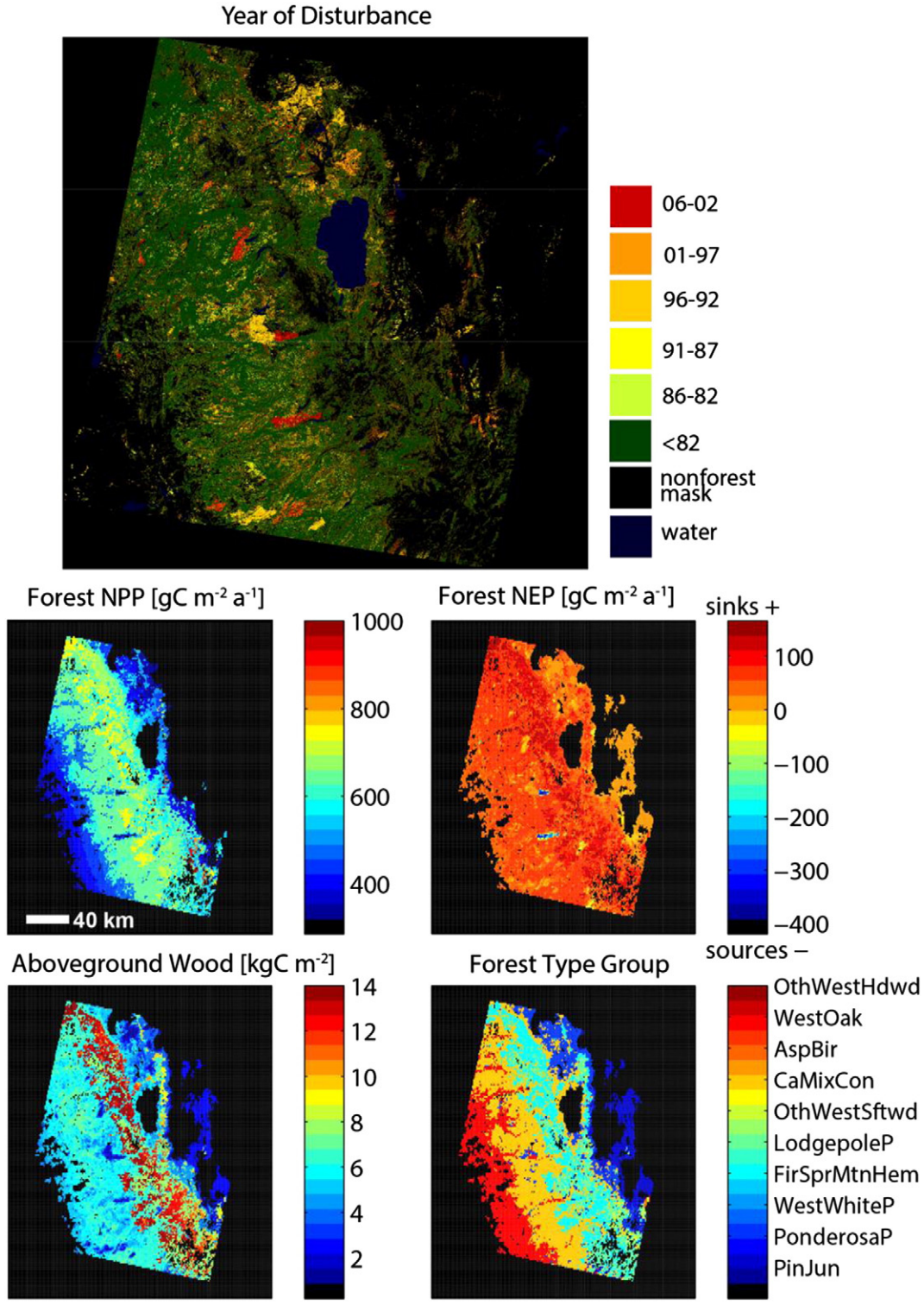

Fig. 6. Same as in Fig. 4 but for Landsat scene p43r33 located in the Sierra Mountains of the Pacific southwest near Tahoe. Fire imposes large patches with similar year of disturbance, also appearing as anomalies in *NPP*, *NEP*, and aboveground wood.

for different contexts. The contemporary forest-atmosphere exchange of carbon dioxide, as represented with *NEP*, is the net near-term uptake (or release) relevant to continental assessments of the current rate at which land sinks are mitigating CO_2 sources from fossil fuel combustion and deforestation, among others. If we compare *NEP* from regrowth alone to *NEP* inferred from the forest stock inventory we also obtain an indirect estimate of the net effect of various global change factors enhancing forest growth and contributing additional carbon sinks (e.g. Williams et al., 2012). On the other hand, the *NEP* perspective discounts both future carbon sequestration as forests grow and future carbon releases as disturbance-killed biomass decomposes either on-site or off-site in wood products. To more fully represent these terms it can be more appropriate to quantify current stocks in live and dead pools and also the potential carbon stocks that might accumulate if

disturbance was avoided for some time into the future. Such calculations of the capacity for future carbon sequestration through forest stock accumulation are misleading because stand-replacing disturbances are in fact an integral part of ecosystem function and will inevitably reduce carbon stocks from this theoretical maximum. Nonetheless, it offers a useful way of illustrating the degree to which carbon stocks are low relative to an upper-bound because of disturbances, principally harvesting. It is also worth noting that areas with greater carbon storage potential achieved that potential from large-area mortality events particularly harvesting practices, and much of the killed biomass is destined for release to the atmosphere (committed emissions). All of these approaches are valuable and relevant and it could be helpful if future work seeks to represent carbon impacts from these multiple perspectives.

Error or missing variance in the stand age at harvesting time could have implications for our carbon balance assessment because the stand age at harvest influences the pre-disturbance biomass subject to harvesting and mortality-induced decomposition and release. To evaluate possible bias we examined the stand age distribution of harvest removals as reported by the EVALIDator web-interface maintained by the FIA for eastern regions (Miles, 2013). About half of all harvested volume was reached by the stand age class of 61–80 years for the Northeast and Northern Lakes States regions, and 21–40 years for the Southeast and South Central regions (Appendix B). While distributions support our general treatment of variability in pre-disturbance ages (typically 75 years but earlier in South Central and Southeast pines and much later for old-growth in the Pacific Northwest), substantial variability remains unaccounted for and future work should seek to represent this variability in carbon balance assessments.

Our accounting framework in this work represented all stand-replacing disturbances with carbon dynamics characteristic of a post-harvest condition. In reality, fire, blowdown, insect damage and other disturbance types are known to account for some of the observed stand-clearings and each imposes a unique post-disturbance carbon legacy. Here we discuss some of the likely implications for continental-scale carbon accounting. All other disturbance agents involve greater post-disturbance carbon releases within forests because killed aboveground biomass is left on-site where it gradually decomposes and is released to the atmosphere. Other disturbance types may also delay *NPP* recovery and delay recruitment of new woody vegetation if top soils are eroded, seed banks are scorched, and snags and coarse woody debris shade the ground more than in the case of a clearing treatment. Locally, this would lower *NEP* in the early years post-disturbance and delay the site's crossover from a within-forest source to a sink of atmospheric CO_2 (referring here to *NEP*). However the effects on *NBP* may be less pronounced as the increase in CO_2 release on-site in forests is compensated by decreased removals. While fires introduce another term of direct emissions from combustion which may accelerate the rate of carbon release of disturbance-killed material as well as some of the detritus present prior to disturbance (Ghimire et al., 2012; Law et al., 2004), harvesting practices can involve similarly prompt emissions when bark, broken or defective wood, and slash is burned with or without energy production either on-site or during primary processing at paper and pulp mills or other wood processing facilities (Harmon, Ferrell, & Franklin, 1990; Skog & Nicholson, 1998). Furthermore, the mean residence time for coarse woody debris is reportedly similar to that for wood products (Harmon et al., 1990). Attributing disturbances to various types and assessing all of their unique impacts are beyond the scope of the current work and should receive attention in future work.

Various sources of uncertainty could bias our regional and conterminous US estimates of the carbon balance impacts of recent forest disturbances. Our method formally propagates two sources of uncertainty including uncertainty in the rate of wood accumulation inferred from FIA age-chronosequences and uncertainty in the area of each forest type group, stand age, and productivity class strata within each method (FIA or RS-FIA). These combine to a standard deviation of about 20% of the mean *NEP* (Table 4). We also report a data source uncertainty regarding the fraction of the landscape that is within young age classes, introducing a *NEP* bias of 6% (Table 4). In our prior work we also reported sensitivity to possible biases in the rate of biomass accumulation with stand age that may be implicit to our use of the FIA data as a constraint on the growth model (Williams et al., 2012, see Auxiliary Material Section 2). Therein we noted sensitivity to partial cutting practices that remove biomass from forested plots of the FIA but do not reset the stand age. If biomass growth was 10% greater than that inferred from the chronosequence, conterminous US forest *NEP* would be elevated by 14% and aboveground biomass would be elevated by 8%. In this work we performed an additional sensitivity test to evaluate possible bias based on assumptions regarding the stand age of harvested forests (Appendix C). Assuming that younger forests are harvested reduces carbon taken offsite, increases *NEP* by reducing on-site carbon emissions from decomposition of disturbance-killed biomass, and thus increases *NBP*. Harvesting of older forests has the opposite effects, increasing carbon taken offsite (Harvest), decreasing *NEP*, and decreasing *NBP*. Assumptions regarding the stand age of harvested forests do not influence the sizeable difference between RS-FIA and FIA-only results. Furthermore, none of the sensitivity results presented here indicates significant movement toward closing the gap we have reported previously (Williams et al., 2012) between the UNFCCC reported rate of carbon uptake in forests and that we derive here based on accounting for the effects of disturbance and regrowth processes. Lastly, as described above, accounting for the unique legacies of non-harvest disturbance types can also be expected to affect our results, likely reducing *NEP* but having more modest effects on carbon stocks and *NBP*.

Further activities are underway to expand and improve the existing analysis presented here. These include the following: 1) developing unique parameterizations for partial disturbances, fire, harvest, and insect damage and applying them based on estimates of disturbance types from data sources such as the Monitoring Trends in Burn Severity dataset for fires and aircraft based estimates of insect outbreaks from the Aerial Detection Survey; 2) utilizing longer time series of Landsat by including pre-1985 Multispectral Scanner data (back to the early 1970's) as well as wall-to-wall sampling across the conterminous US. The current (third) phase of the NAFD project is implementing a wall-to-wall, annual mapping of forest disturbance across the United States which should help avoid the concern of spatial sampling bias that arises for this current 54-scene analysis. This approach will mitigate the sampling biases for specific forest types, provide greater sensitivity to partial disturbances, and will also include the attribution of disturbance type. Other parallel research efforts (e.g. Duane et al., 2010; Ohmann & Gregory, 2002) are seeking to describe stand age even beyond that mapped directly from spectral change detection methods and if available at the continental scale would provide a valuable extension enabling additional spatial detail for all forests not just those recently disturbed; 3) expanding the representation of carbon pools in the model to include fine (branches) and coarse (trunks and standing dead) wood and CWD with unique turnover rates, as this is especially important for capturing the slow turnover of standing dead wood after fire as well as in very dry environments; and, 4) evaluating predicted regional to national scale disturbance fluxes using top-down analysis of atmospheric CO_2 variability in collaboration with atmospheric transport modelers.

5. Conclusions

The Landsat record provides detailed information about disturbance history, used here to identify forest age and associated carbon stocks and fluxes. When combined with forest inventory data to constrain biomass accumulation rates in a carbon cycle model, the integrated method

provides a data-rich, process-specific, and novel approach to estimating regional and country-scale carbon stocks and fluxes as they respond to disturbance, forest type, and climate patterns. Large variation in disturbance rates is found both within and between regions, partly explained by large-scale patterns of harvest management and diversity of forest types and climate settings. Rates also vary by method, with remotely sensed disturbance rates generally exceeding those inferred from stand ages reported in the inventory data. Naturally, regions experiencing high disturbance rates have the greatest potential to sequester carbon lost from disturbance as forests regrow. Most notably this includes the South Central, Pacific Northwest, and Rocky Mountain North regions. Despite lower contemporary disturbance rates, the Northeast remains a strong carbon sink with significant potential to sequester additional carbon through forest regrowth. Observations and methodological advances are still needed to more fully represent the diversity of impacts from different disturbance types and severities as well as variations in carbon residence times in different ecosystem pools.

Acknowledgments

We thank Charles (Chip) Scott and his team at the USFS National Inventory and Monitoring Applications Center for providing us with FIA data. We acknowledge the helpful discussions and comments from Warren Cohen, Richard Houghton, Nancy Thomas, Karen Schleeweis, Robert Kennedy, Scott Powell, Sean Healey, and Gretchen Moisen, as well as from five anonymous reviewers. We would also like to thank the organizers of this Special Issue, including Warren Cohen, Ronald McRoberts, and Dirk Pflugmacher, for giving us the opportunity to contribute following the ForestSAT 2012 Conference. This work was funded by NASA NNH05ZDA001N, North American Carbon Program.

Appendix A. States and years included in each region's sample of FIA data via the TabGen interface

Northeast

Connecticut: Cycle; EVALID = 90601; Years 1985, 1998, 2003, 2004, 2005, 2006.

Maine: Cycle; EVALID = 230601; Years 1995, 1999, 2000, 2001, 2002, 2003, 2004, 2005, 2006.

Maryland: Cycle; EVALID = 240601; Years 1986, 1999, 2004, 2005, 2006.

Massachusetts: Cycle; EVALID = 250601; Years 1985, 1998, 2003, 2004, 2005, 2006.

New Hampshire: Cycle; EVALID = 330601; Years 1983, 1997, 2002, 2003, 2004, 2005, 2006.

New Jersey: Cycle; EVALID = 340601; Years 1987, 1999, 2004, 2006, 2005.

New York: Cycle; EVALID = 360601; Years 1993, 2002, 2003, 2004, 2005, 2006.

Pennsylvania: Cycle 5; EVALID = 420601; Years 1989, 2000, 2001, 2002, 2003, 2004, 2005, 2006.

Rhode Island: Cycle; EVALID = 440601; Years 1985, 1998, 2003, 2004, 2005, 2006.

Vermont: Cycle; EVALID = 500601; Years 1983, 1997, 2003, 2004, 2005, 2006.

West Virginia: Cycle; EVALID = 540601; Years 1989, 2000, 2004, 2005, 2006.

Northern Lakes States

Michigan: Cycle; EVALID = 260601; Years 1980, 1993, 2000, 2001, 2002, 2003, 2004, 2005, 2006.

Minnesota: Cycle; EVALID = 270701; Years 1977, 1990, 1999, 2000, 2001, 2002, 2003, 2004, 2005, 2006, 2007.

Wisconsin: Cycle 7; EVALID = 550701; Years 1983, 1996, 2000, 2001, 2002, 2003, 2004, 2005, 2006, 2007.

Northern Prairie States

Illinois: Cycle; EVALID = 170601; Years 1985, 1998, 2001, 2002, 2003, 2004, 2005, 2006.

Indiana: Cycle; EVALID = 180701; Years 1986, 1998, 1999, 2000, 2001, 2002, 2003, 2004, 2005, 2007, 2006.

Iowa: Cycle; EVALID = 190601; Years 1990, 1999, 2000, 2001, 2002, 2003, 2004, 2005, 2006.

Kansas: Cycle; EVALID = 200601; Years 1981, 1994, 2001, 2002, 2003, 2004, 2005, 2006.

Missouri: Cycle; EVALID = 290601; Years 1989, 1999, 2000, 2001, 2002, 2003, 2004, 2005, 2006.

Nebraska: Cycle 4; EVALID = 310601; Years 1983, 1994, 2001, 2002, 2003, 2004, 2005, 2006.

North Dakota: Cycle; EVALID = 380601; Years 1980, 1995, 2001, 2002, 2003, 2004, 2005, 2006.

Ohio: Cycle; EVALID = 390601; Years 1991, 2001, 2002, 2003, 2004, 2005, 2006.

South Dakota: Cycle; EVALID = 460601; Years 1980, 1995, 2001, 2002, 2003, 2004, 2005, 2006.

Pacific Southwest

California: Cycle 5; EVALID = 5; Years 2001, 2002, 2003, 2004, 2005, 2006, 2007.

Pacific Northwest

Oregon: Cycle; EVALID = 4; Years 1992, 2001, 2002, 2003, 2004, 2005, 2006, 2007.

Washington: Cycle 5; EVALID = 6; Years 1991, 2002, 2003, 2004, 2005, 2006, 2007.

Rocky Mountain North

Idaho: Cycle; EVALID = 160701; Years 1991, 1999, 2004, 2005, 2006, 2007.

Montana: Cycle 1; EVALID = 300701; Years 1989, 1999, 2003, 2004, 2005, 2006, 2007.

Rocky Mountain South

Arizona: Cycle; EVALID = 40701; Years 1985, 1999, 2001, 2002, 2003, 2004, 2005, 2006, 2007.

Colorado: Cycle; EVALID = 80701; Years 1984, 1999, 2002, 2003, 2004, 2005, 2006, 2007.

New Mexico: Cycle; EVALID = 359902; Years 1987, 1999.

Utah: Cycle; EVALID = 490701; Years 1993, 1999, 2000, 2001, 2002, 2003, 2004, 2005, 2006, 2007.

Wyoming: Cycle 2; EVALID = 560002; Years 1984, 2000.

South Central

Alabama: Cycle; EVALID = 10701; Years 1990, 2000, 2001, 2002, 2003, 2004, 2005, 2006, 2007.

Arkansas: Cycle; EVALID = 50701; Years 1995, 2000, 2002, 2003, 2005, 2004, 2006, 2007.

Kentucky: Cycle; EVALID = 210601; Years 1988, 1999, 2000, 2001, 2002, 2003, 2004, 2005, 2006.

Louisiana: Cycle; EVALID = 220501; Years 1991, 2001, 2002, 2003, 2004, 2005.

Mississippi: Cycle; EVALID = 280601; Years 1994, 2006.

Oklahoma: Cycle; EVALID = 409302; Years 1993, 1989.

Tennessee: Cycle 8; EVALID = 470601; Years 1989, 1999, 2000, 2001, 2002, 2004, 2003, 2005, 2006.

Texas: Cycle; EVALID = 480701; Years 1992, 2001, 2002, 2003, 2004, 2005, 2006, 2007.

Southeast

Florida: Cycle; EVALID = 120601; Years 1987, 1995, 2003, 2004, 2005, 2006.

Georgia: Cycle; EVALID = 130601; Years 1989, 1997, 1998, 2000, 2003, 2002, 2001, 1999, 2004, 2005, 2006.

North Carolina: Cycle; EVALID = 370601; Years 1984, 1990, 2002, 2003, 2004, 2005, 2006.

South Carolina: Cycle; EVALID = 450602; Years 1986, 1993, 1999, 2000, 2001, 2002, 2003, 2004, 2005, 2006.

Virginia: Cycle 8; EVALID = 510701; Years 1984, 1992, 1998, 1999, 2000, 2001, 2002, 2003, 2005, 2006, 2007.

Appendix B. Stand age distribution of harvest removals for eastern US regions

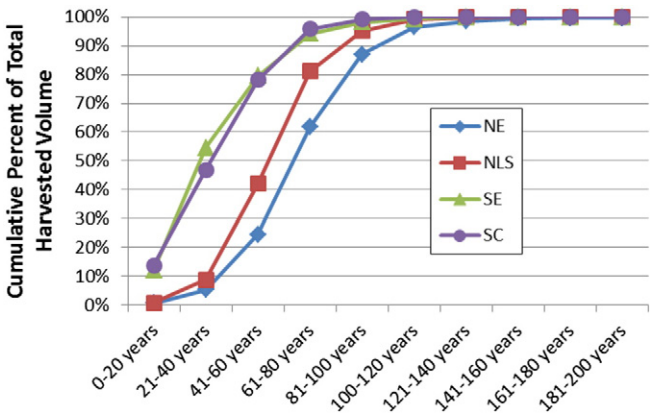

Fig. B1. Cumulative frequency distribution of harvested volume by stand age class based on a data sample from the US FIA database sampled with EVALIDator (Miles, 2013) for all states and forest types within four regions.

Miles, P.D. (2013). Forest Inventory EVALIDator web-application version 1.5.1.05. St. Paul, MN: U.S. Department of Agriculture, Forest Service, Northern Research Station. [Available only on internet: http://apps.fs.fed.us/Evalidator/tmattribute.jsp]

Appendix C. Sensitivity to pre-disturbance stand age

The table below reports results from a sensitivity study in which we adjusted the age of harvested stands to be younger or older than that assumed in the main work. In the original work we assumed all forests to be harvested at a stand age of 75 years old except for Douglas fir forests (200 years old) or loblolly, shortleaf, longleaf, and slash pines (30 years old). We also tested how results change if we assume 95, 200, and 50 year old pre-harvest stand ages (*Old* scenario), or 55, 80, and 30 year old pre-harvest stand ages (*Young* scenario), where ages correspond to all forests, except for Douglas fir, and select pine types, respectively.

Net ecosystem productivity and harvest removals are sensitive to the pre-disturbance age of harvested forests. This is because the amount of harvest-killed biomass and corresponding post-disturbance decomposition on site are strongly linked to pre-disturbance biomass stocks which are themselves influenced by stand age. Harvesting of younger forests reduces carbon taken offsite (Harvest) and increases *NEP* by reducing on-site carbon emissions from decomposition of disturbance-killed biomass. Harvesting younger forests thus increases *NBP*. Harvesting of older forests has the opposite effects, increasing carbon taken offsite (Harvest), decreasing *NEP*, and decreasing *NBP*. Assumptions regarding the stand age of harvested forests do not influence the sizeable difference between RS-FIA and FIA-only results, which remains fairly constant regardless of the pre-disturbance stand age that is assumed. Furthermore, none of the sensitivity results presented here indicates significant movement toward closing the gap between the UNFCCC reported rate of carbon uptake in forests and that we derive here based on accounting for the effects of disturbance and regrowth processes.

References

Allen, C. D., Macalady, A. K., Chenchouin, H., Bachelet, D., McDowell, N., Vennetier, M., et al. (2010). A global overview of drought and heat-induced tree mortality reveals emerging climate change risks for forests. *Forest Ecology and Management*, *259*, 660–684.

Amiro, B.D., Chen, J. M., & Liu, J. (2000). Net primary productivity following forest fire for Canadian ecoregions. *Canadian Journal of Forest ResearchRevue Canadienne De Recherche Forestiere*, *30*, 939–947.

Bechtold, W. A., & Patterson, P. L. (2005). *The enhanced Forest Inventory and Analysis program—national sampling design and estimation procedures, SRS GTR-80.* Asheville, North Carolina, USA: USDA Forest Service, Southern Research Station.

Binford, M., Gholz, H., Starr, G., & Martin, T. (2006). Regional carbon dynamics in the southeastern U.S. coastal plain: Balancing land cover type, timber harvesting, fire, and environmental variation. *Journal of Geophysical Research–Biogeosciences*, *111*, D24S92, http://dx.doi.org/10.1029/2005JD006820.

Bradford, J. B., Birdsey, R. A., Joyce, L. A., & Ryan, M. G. (2008). Tree age, disturbance history, and carbon stocks and fluxes in subalpine Rocky Mountain forests. *Global Change Biology*, *14*, 2882–2897.

Chapin, F. S., III, Woodwell, G. M., Randerson, J. T., Rastetter, E. B., Lovett, G. M., Baldocchi, D. B., et al. (2006). Reconciling carbon-cycle concepts, terminology, and methods. *Ecosystems*, *9*, 1041–1050.

Cohen, W., Harmon, M., Wallin, D. O., & Fiorella, M. (1996). Two decades of carbon flux from forests of the Pacific Northwest. *BioScience*, *46*, 836–844.

Cohen, W., Spies, T., Alig, R., Oetter, D., Maiersperger, T., & Fiorella, M. (2002). Characterizing 23 years (1972–95) of stand replacement disturbance in western Oregon forests with Landsat imagery. *Ecosystems*, *5*, 122–137.

Cohen, W., Spies, T., & Fiorella, M. (1995). Estimating the age and structure of forests in a multi-ownership landscape of western Oregon, USA. *International Journal of Remote Sensing*, *16*, 721–746.

Duane, M. V., Cohen, W. B., Campbell, J. L., Hudiburg, T., Weyermann, D., & Turner, D. P. (2010). Implications of two different field-sampling designs on landsat-based forest age maps used to model carbon in Oregon forests. *Forest Science*, *65*, 405–416.

Eidenshink, J., Schwind, B., Brewer, K., Zhu, Z. -L., Quayle, B., & Howard, S. (2007). A project for monitoring trends in burn severity. *Fire Ecology*, *3*, 3–21.

Ghimire, B., Williams, C. A., Collatz, G. J., & Vanderhoof, M. E. (2012). Fire-induced carbon emissions and regrowth uptake in western U.S. forests: Documenting variation across forest types, fire severity, and climate regions. *Journal of Geophysical Research*, *117*, G03036.

Goetz, S. J., Bond-Lamberty, B., Law, B. E., Hicke, J. A., Huang, C., Houghton, R. A., et al. (2012). Observations and assessment of forest carbon dynamics following disturbance in North America. *Journal of Geophysical Research*, *117*, G02022.

Goward, S. N., Huang, C., Masek, J. G., Cohen, W. B., Moisen, G. G., & Schleeweis, K. (2012). *NACP North American Forest Dynamics Project: Forest Disturbance and Regrowth Data.* Oak Ridge, Tennessee, U.S.A.: ORNL DAAC, http://dx.doi.org/10.3334/ORNLDAAC/1077 (Available on-line [http://daac.ornl.gov] from)

Table C1
Regional results for net ecosystem productivity (*NEP*), annual harvest removals (Harvest), and net biome productivity (*NBP* = *NEP* – Harvest) for the *Young* and *Old* stand ages just prior to harvesting. Subheadings RS and FIA refer to results when age distributions are estimated either with or without the NAFD 54-scene Landsat product.

Region	NEP				Harvest				NBP			
	RS		FIA		RS		FIA		RS		FIA	
	Young	Old	Young	Old	Young	Old	Young	Old	Young	Old	Young	Old
NE	34	29	36	32	17	22	7	9	17	7	29	23
NLS	12	10	12	11	7	9	4	6	5	1	8	5
SE	32	23	31	23	25	32	28	36	7	−9	3	−13
SC	38	31	38	30	34	45	34	45	4	−14	4	−15
RMN	5	4	7	6	13	18	8	11	−8	−14	−1	−5
RMS	9	9	10	11	9	12	7	10	0	−3	3	1
PSW	11	10	13	12	7	10	3	4	4	0	10	8
PNW	18	10	21	13	17	24	16	23	1	−14	5	−10
Total	159	128	168	138	129	172	108	143	30	−44	60	−5

Goward, S. N., Masek, J. G., Cohen, W., Moisen, G., Collatz, G. J., Healey, S., et al. (2008). Forest disturbance and North American carbon flux. *EOS. Transactions of the American Geophysical Union*, *89*, 105–106.

Harmon, M. E., Ferrell, W. K., & Franklin, J. F. (1990). Effects on carbon storage of conversion of old-growth forests to young forests. *Science*, *247*, 699–702.

Harmon, M. E., Franklin, J. F., Swanson, F. J., Sollins, P., Gregory, S. V., Lattin, J.D., et al. (1986). Ecology of coarse woody debris in temperate ecosystems. *Advances in Ecological Research*, *15*, 133–288.

Hicke, J. A., Asner, G. P., Kasischke, E. S., French, N. H. F., Randerson, J. T., Collatz, G. J., et al. (2003). Postfire response of North American boreal forest net primary productivity analyzed with satellite observations. *Global Change Biology*, *9*, 1145–1157.

Houghton, R. A., & Hackler, J. L. (2000). Changes in terrestrial carbon storage in the United States. 1: The roles of agriculture and forestry. *Global Ecology and Biogeography*, *9*, 125–144.

Huang, C., Goward, S. N., Masek, J. G., Gao, F., Vermote, E. F., Thomas, N., et al. (2009a). Development of time series stacks of Landsat images for reconstructing forest disturbance history. *International Journal of Digital Earth*, *2*, 195–218.

Huang, C., Goward, S. N., Masek, J. G., Thomas, N., Zhu, Z., & Vogelmann, J. E. (2010a). An automated approach for reconstructing recent forest disturbance history using dense Landsat time series stacks. *Remote Sensing of Environment*, *114*, 183–198.

Huang, C., Goward, S. N., Schleeweis, K., Thomas, N., Masek, J. G., & Zhu, Z. (2009b). Dynamics of national forests assessed using the Landsat record: Case studies in eastern U.S. *Remote Sensing of Environment*, *113*, 1430–1442.

Huang, C., Thomas, N., Goward, S. N., Masek, J. G., Zhu, Z., Townshend, J., et al. (2010b). Automated masking of cloud and cloud shadow for forest change analysis. *International Journal of Remote Sensing*, *31*, 5464–5549.

IPCC (2000). Intergovernmental Panel on Climate Change Good Practice Guidance and Uncertainty Management in National Greenhouse Gas Inventories. In J. Penman, D. Kruger, I. Glbally, T. Hiraishi, B. Nyenzi, S. Emmanul, L. Buendia, R. Hoppaus, T. Martinsen, J. Meijer, K. Miwa, & K. Tanabe (Eds.), Japan: Institute for Global Environmental Strategies.

Kennedy, R. E., Cohen, W. B., & Schroeder, T. A. (2007). Trajectory-based change detection for automated characterization of forest disturbance dynamics. *Remote Sensing of Environment*, *110*, 370–386.

Laiho, R., & Prescott, C. E. (2004). Decay and nutrient dynamics of coarse woody debris in northern coniferous forests: A synthesis. *Canadian Journal of Forest ResearchRevue Canadienne De Recherche Forestiere*, *34*, 763–777.

Law, B. E., Turner, D., Campbell, J. L., Van Tuyl, S., Ritts, W. D., & Cohen, W. B. (2004). Disturbance and climate effects on carbon stocks and fluxes across Western Oregon USA. *Global Change Biology*, *10*, 1429–1444.

Masek, J. G., & Collatz, G. J. (2006). Estimating forest carbon fluxes in a disturbed southeastern landscape: Integration of remote sensing, forest inventory, and biogeochemical modeling. *Journal of Geophysical Research*, *111*, G01006.

Masek, J. G., Goward, S. N., Kennedy, R., Cohen, W. B., Moisen, G., Schleweiss, K., et al. (2013). U.S. forest disturbance trends observed with Landsat time series. *Ecosystems*, 1–18.

Masek, J. G., Huang, C., Wolfe, R., Cohen, W., Hall, F., Kutler, J., et al. (2008). North American forest disturbance mapped from a decadal Landsat record. *Remote Sensing of Environment*, *112*, 2914–2926.

Masek, J. G., Vermote, E. F., Saleous, N. E., Wolfe, R., Hall, F. G., Huemmrich, K. F., et al. (2006). A Landsat surface reflectance dataset for North America, 1990–2000. *IEEE Geoscience and Remote Sensing Letters*, *3*, 68–72.

Miles, P. D. (2013). Forest Inventory EVALIDator web-application version 1.5.105. In F.S. U.S. Department of Agriculture, Northern Research Station (Ed.), [Available only on internet: http://apps.fs.fed.us/Evalidator/tmattribute.jsp], St. Paul, MN

Ohmann, J. L., & Gregory, M. J. (2002). Predictive mapping of forest composition and structure with direct gradient analysis and nearest-neighbor imputation in coastal Oregon, U.S.A. *Canadian Journal of Forest ResearchRevue Canadienne De Recherche Forestiere*, *32*, 725–741.

Potter, C. S., Randerson, J. T., Field, C. B., Matson, P. A., Vitousek, P.M., Mooney, H. A., et al. (1993). Terrestrial ecosystem production — a process model-based on global satellite and surface data. *Global Biogeochemical Cycles*, *7*, 811–841.

Powell, D. S., Faulkner, J. K., Darr, D. R., Zhiliang, Z., & MacCleery, D. W. (1993). *Forest resources of the United States, 1992.* General Technical Report RM-GTR-234 [Revised, June 1994]. Fort Collins, CO: U.S. Department of Agriculture, Forest Service, Rocky Mountain Forest and Range Experiment Station (132 pp. + map. In).

Randerson, J. T., Thompson, M. V., Malmstrom, C. M., Field, C. B., & Fung, I. Y. (1996). Substrate limitations for heterotrophs: Implications for models that estimate the seasonal cycle of atmospheric CO_2. *Global Biogeochemical Cycles*, *10*, 585–602.

Ruefenacht, B., Finco, M. V., Nelson, M.D., Czaplewski, R., Helmer, E. H., Blackard, J. A., et al. (2008). Conterminous U.S. and Alaska forest type mapping using Forest Inventory and Analysis Data. *Photogrammetric Engineering and Remote Sensing*, *74*, 1379–1388.

Schroeder, T. A., Cohen, W. B., & Yang, Z. (2007). Patterns of forest regrowth following clearcutting in western Oregon as determined from a Landsat time-series. *Forest Ecology and Management*, *243*, 259–273.

Scott, C. T., Bechtold, W. A., Reams, G. A., Smith, W. D., Westfall, J. A., Hansen, M. H., et al. (2005). Sample-based estimators used by the Forest Inventory and Analysis National Information Management System. In W. A. Bechtold, & P. L. Patterson (Eds.), *The enhanced Forest Inventory and Analysis program—national sampling design and estimation procedures. USDA Forest Service, Southern Research Station, General Technical Report SRS-80* (pp. 43–67) (Asheville, NC).

Skog, K., & Nicholson, G. A. (1998). Carbon cycling through wood products: The role of wood and paper products in carbon sequestration. *Forest Products Journal*, *48*, 75–83.

Smith, J. E., & Heath, L. S. (2001). Identifying influences on model uncertainty: An application using a forest carbon budget model. *Environmental Management*, *27*, 253–267.

Smith, W. B., Miles, P. D., Perry, C. H., Pugh, S. A., & Forest Resources of the United States, 2007 (2009). *Forest Resources of the United States.* Gen. Tech. Rep. WO-78. Washington, DC: USDA, Forest Service, Washington Office (336 pp.).

Song, C., & Woodcock, C. E. (2003). A regional forest ecosystem carbon budget model: Impacts of forest age structure and land use history. *Ecological Modelling*, *164*, 33–47.

Taylor, J. R. (1997). *An introduction to error analysis: The study of uncertainties in physical measurements* (2nd ed.)Sausilito, California: University Science Books.

Thomas, N. E., Huang, C., Goward, S. N., Powell, S., Rishmawi, K., Schleeweis, K., et al. (2011). Validation of North American Forest Disturbance dynamics derived from Landsat time series stacks. *Remote Sensing of Environment*, *115*, 119–132.

Turner, D. P., Koerper, G. J., Harmon, M. E., & Lee, J. J. (1995). A carbon budget for forests of the conterminous United States. *Ecological Applications*, *5*, 421–436.

Turner, D. P., Ritts, W. D., Law, B. E., Cohen, W. B., Yang, Z., Hudiburg, T., et al. (2007). Scaling net ecosystem production and net biome production over a heterogeneous region in the western United States. *Biogeosciences*, *4*, 597–612.

Vermote, E. F., Tanre, D., Deuze, J. L., Herman, M., & Morcrette, J. J. (1997). Second simulation of the satellite signal in the solar spectrum, 6 s: An overview. *IEEE Geoscience and Remote Sensing Letters*, *35*, 675–686.

Williams, C. A., Collatz, G. J., Masek, J. G., & Goward, S. (2012). Carbon consequences of forest disturbance and recovery across the conterminous United States. *Global Biogeochemical Cycles*, *26*, GB1005.

Zaehle, S., Sitch, S., Prentice, I. C., Liski, J., Cramer, W., Erhard, M., et al. (2006). The importance of age-related decline in forest NPP for modeling regional carbon balances. *Ecological Applications*, *16*, 1555–1574.